Published February 25, 2013, doi:10.4049/jimmunol.1203086

IRF7-Dependent IFN-β Production in Response to RANKL Promotes Medullary Thymic Epithelial Cell Development

Dennis C. Otero,*,† Darren P. Baker,‡ and Michael David*,†

The contributions of IFN regulatory factor (IRF) 3/7 and the type I IFNs IFN-α/β to the innate host defense have been extensively investigated; however, their role in thymic development is less clear. In this study, we show that mice lacking the type I IFN receptor IFN-α/β receptor (IFNAR) or the downstream transcription factor STAT1 harbor a significant reduction in self-Ag–presenting, autoimmune regulator (AIRE)$^+$ medullary thymic epithelial cells (mTECs). Constitutive IFNAR signaling occurs in the thymic medulla in the absence of infection or inflammation. Receptor activator for NF-κB (RANK) ligand stimulation results in IFN-β upregulation, which in turn inhibits RANK signaling and facilitates AIRE expression in mTECs. Finally, we find that IRF7 is required for thymic IFN-β induction, maintenance of thymic architecture, and mTEC differentiation. We conclude that spatially and temporally coordinated cross talks between the RANK ligand/RANK and IRF7/IFN-β/IFNAR/STAT1 pathways are essential for differentiation of AIRE$^+$ mTECs. ***The Journal of Immunology*****, 2013, 190: 000–000.**

Selection of Ag receptor–expressing T lymphocytes that are MHC restricted but tolerant to self-Ags is an essential prerequisite for a functional immune system. Of vital importance to this process of central tolerance in the thymus is medullary thymic epithelial cells (mTECs) that are characterized by promiscuous gene expression of self-Ag. The autoimmune regulator (AIRE) is responsible for the expression of otherwise tissue-specific Ag (TSA) in mTECs and is necessary for T cell tolerance and prevention of autoimmunity (1, 2). Mutations in the gene encoding AIRE in humans results in development of autoimmune polyendocrinopathy-candidiasis-ectodermal dystrophy (3), a multiorgan autoimmune disease characterized by multiple adrenal system defects including hypothyroidism and adrenal insufficiency as well as susceptibility to yeast infection (candidiasis) (4). Mice deficient in AIRE expression reproduce many of the defects observed in human autoimmune polyendocrinopathy-candidiasis-ectodermal dystrophy (5). The development of AIRE-expressing mTECs is governed by several TNF family members, including receptor activator for NF-κB (RANK), CD40, and lymphotoxin β (LTβ) (6–9). Defects in their respective receptors or signaling components (RelB, NIK, or TNFR-associated factor 6) result in a reduced or absent medullary region in the thymus and development of autoimmunity in mutant mice (10–12). Thus, the proper development of AIRE-expressing mTECs is required for the maintenance of an intact thymic architecture and consequently of T cell tolerance to self-Ag.

STAT1 is a well-defined element of the type I (IFN-α/β) and type II (IFN-γ) IFN-induced signaling cascades (13–15). The physiological significance of STAT1 in vivo has been elucidated through the generation of STAT1-deficient mice by two independent laboratories (16, 17). As predicted, STAT1-deficient mice are impaired in responses to either type I or type II IFNs; however, analysis of the specific T cell subpopulation in wild-type (WT) and STAT1$^{-/-}$ mice provided no indication for significant differences between these two strains (16–18).

Even though all IFNs use STAT1 as a signaling intermediary, type I and II IFNs elicit opposing effects on the progression of the demyelinating, T cell–mediated autoimmune disease multiple sclerosis (MS) (19). These contrasting effects of IFN-α/β and IFN-γ in MS prompt the question as to the role of STAT1 in this pathological process. To investigate this matter, we had previously used mice carrying a transgenic TCR specific for myelin basic protein (TCR^{MBP}). Upon immunization with MBP, TCR^{MBP} mice develop experimental autoimmune encephalomyelitis (EAE), which serves as a murine model for MS (20, 21). The dramatically increased susceptibility to EAE development of TCR^{MBP}STAT1-deficient mice is accounted for, at least in part, by a defect in the development and functionality of CD4$^+$CD25$^+$ regulatory T cells (T_{reg}) (18). However, the severity and frequency of spontaneous EAE development in the absence of STAT1 suggested that STAT1 might also be a factor in thymic events that control central tolerance. We recently reported that TCR-transgenic STAT1$^{-/-}$ and IFN-α/β receptor (IFNAR)$^{-/-}$, but not IFN-γ receptor (IFNGR)$^{-/-}$ animals, displayed striking differences in T cell selection compared with WT littermates (22).

Our current studies illustrate that IFN regulatory factor (IRF) 7, IFNAR1, and STAT1, but not type II IFN, are essential for the development of mTECs and maintenance of thymic architecture, both in the presence and absence of transgenic TCR expression. Additional investigations corroborated constitutive type I IFN responses in the absence of infections that are restricted to the

*Division of Biological Sciences, University of California, San Diego, La Jolla, CA 92093; †UC San Diego Moores Cancer Center, University of California, San Diego, La Jolla, CA 92093; and ‡Biogen Idec, Cambridge, MA 02142

Received for publication November 7, 2012. Accepted for publication January 24, 2013.

This work was supported by National Institutes of Health/National Institute of Allergy and Infectious Diseases Grant AI71223 and funding from the National Multiple Sclerosis Society (54109A to M.D.).

Address correspondence and reprint requests to Dr. Michael David, University of California, San Diego, Division of Biological Sciences, Molecular Biology Section, Bonner Hall 3138, 9500 Gilman Drive, La Jolla, CA 92093-0322. E-mail address: midavid@ucsd.edu

The online version of this article contains supplemental material.

Abbreviations used in this article: AIRE, autoimmune regulator; cTEC, cortical thymic epithelial cell; EAE, experimental autoimmune encephalomyelitis; EpCAM, epithelial cell adhesion molecule; IFNAR, IFN-α/β receptor; IFNGR, IFN-γ receptor; IRF, IFN regulatory factor; K5, keratin 5; K8, keratin 8; LTβ, lymphotoxin β; MHC II, MHC class II; MS, multiple sclerosis; mTEC, medullary thymic epithelial cell; RANK, receptor activator for NF-κB; RANKL, receptor activator for NF-κB ligand; RFP, red fluorescence protein; TCR^{MBP}, TCR specific for myelin basic protein; T_{reg}, regulatory T cell; UEA-1, *Ulex europaeus* agglutinin-1; WT, wild-type; YFP, yellow fluorescent protein.

thymic medulla and established a cross talk between the RANK and IFN signaling cascades crucial for the development of AIRE-expressing mTECs.

In summary, our findings endorse the notion that the type I IFN system influences thymic structure and function and consequently affects T cell selection by promoting the development of mTECs, a process that involves the temporally and spatially coordinated interplay between the RANK and IFN signaling pathways.

Materials and Methods

Animals and cell culture

STAT1$^{-/-}$ (17), IFNAR1$^{-/-}$ (23), IRF3$^{-/-}$ (24), and IRF7$^{-/-}$ (25) mice have been described previously. Transgenic Mx1-Cre mice and mT/mG mice were obtained from The Jackson Laboratory (Bar Harbor, ME). Animals were between 6 and 10 wk of age at the time of the experiments. All mice used in these experiments were housed in a pathogen-free environment and bred and cared for in accordance with University of California, San Diego Animal Care Facility regulations. All studies involving animal have been approved by the University of California, San Diego Animal Subject Committee (Protocol S02194). The mTEC cell line TE-71 was generously provided by Dr. A. Farr and cultured in DMEM plus 10% FBS.

Flow cytometric analysis

For immunostaining, single-cell suspensions were prepared from thymi with ~10^6 cells suspended in FACS buffer (PBS [pH 7.4], 1% FCS, and 0.02% NaN_3) and stained for 20 min in the dark on ice. APC–anti-CD4 (GK1.5), FITC–anti-MHC II (M5/114.15.2), PE–anti-RANKL (IK22/5), PE/Cy7–anti-CD8 (53.6.7), PE/Cy7 anti-CD45 (30-F11) and PE–anti-CD80 were obtained from eBioscience (San Diego, CA). Biotin–anti-CD11c (HL3), biotin–anti-rat IgG2a (RG7/1.30), and purified anti-EpCAM (G8.8) were obtained from BD Biosciences (San Jose, CA). APC-streptavidin was used as a secondary reagent to detect biotin-labeled mAbs. All samples were analyzed on an FACSCalibur (BD Biosciences) and processed using CellQuest software (BD Biosciences) or Flow Jo (Tree Star, Ashland, OR).

Immunohistochemistry

Paraformaldehyde-fixed 6-μm frozen sections were blocked with 1% FBS in PBS (pH 7.4) for 20 min before staining with the indicated Abs for 2 h or overnight: biotin-labeled *Ulex europaeus* agglutinin-1 (UEA-1; Vector Laboratories, Burlingame, CA), anti-AIRE (Santa Cruz, Santa Cruz, CA), keratin 5 (K5; Covance, Emeryville, CA), and EpCAM (G8.8; BD Biosciences). SA-FITC or SA-APC (eBioscience) and anti-rabbit Ig Cy3 (Jackson ImmunoResearch Laboratories, West Grove, PA) were used as secondary Abs. Images were captured on a CRI Nuance Multispectral Imaging (Caliper, Hopkinton, MA) system attached to a Nikon E800 fluorescent microscope (Nikon). Numbers of AIRE-positive cells were determined from six sections cut from the center of the thymus, discarding 20 μm between each section, from 6–8-wk-old WT or STAT1$^{-/-}$ mice.

Thymocyte stimulation

Splenic T cells or thymocytes were stimulated with the indicated concentrations of IFN-β (Biogen Idec, Cambridge, MA) for 30 min, and cells were lysed in and subjected to SDS-PAGE and Western blot. Blots were probed for phospho-STAT1 and STAT1 (Cell Signaling Technology). Thymocytes from TCR^{OTII} or TCR^{OTII} STAT1$^{-/-}$ mice were stimulated for 24 h by addition to wells containing thymic stromal cells as APCs that were loaded with $OVA_{323–339}$ peptide. Cells were then stained for RANK ligand (RANKL) expression using anti-mRANKL PE (eBioscience) and analyzed by flow cytometry.

mTEC isolation and stimulation

Thymic stromal cells from WT or STAT1$^{-/-}$ mice were purified as described (1). Briefly, thymi were cut into ~1-mm pieces and digested with collagenase/dispase (Sigma-Aldrich, St. Louis, MO) to generate single-cell suspensions, and stromal cells were enriched over a Percoll gradient (GE Healthcare, Piscataway, NJ). CD45$^-$ stromal cells were analyzed by flow cytometry for mTEC markers or stimulated with 500 ng/ml RANKL and/or 1000 U/ml recombinant, Chinese hamster ovary cell–expressed, murine IFN-β (Biogen Idec) for the indicated times. Quantitative RT-PCR was carried out on TRIzol (Sigma-Aldrich) purified mRNAs from stimulated stromal cells and analyzed for the expression of IFN-β using the following primers 5′-CTG AAT GGA AAG ATC AAC CTC AC-3′ and 5′-TAC CTT TGC ACC CTC CAG TAA TA-3′. TaqMan Gene Expression Assays were used for AIRE, INS2, and CRP (Applied Biosystems, Carlsbad, CA). Analysis was carried out on an ABI Prism 7000 (Applied Biosystems).

Results

Reduced medullary region in thymi of IFNAR1- or STAT1-deficient mice

We previously reported that mice deficient for STAT1 and IFNAR1, but not IFNGR, display defective deletion of autoreactive thymocytes. As mTECs are a crucial element in this process, we contemplate IFN-α/β might be playing a role in mTEC development. Abnormal thymic structure has been described previously in mice that contain mutations in particular signaling pathways such as LTβ receptor, RANK, and CD40 (7, 8, 26). Taking into consideration that STAT1-deficient animals had shown similar susceptibility to autoimmune disease as the above mice, we decided to analyze the thymic architecture in STAT1-deficient non-TCR–transgenic mice. H&E staining of thymic sections from STAT1$^{-/-}$ mice revealed a reduced medullary region in the thymic lobe as compared with WT mice (Fig. 1A, *left panel*). This was further confirmed by immunofluorescence staining of thymic sections for K5, a cell-surface marker highly expressed in immature mTECs, and to a significantly lesser extent in mature mTECs (27) (Fig. 1A, *center left panel*). A reduced ratio of medullary to cortical area in thymi of STAT1$^{-/-}$ mice was revealed in several sections from multiple mice (Fig. 1B, quantitated in Fig. 1C). In addition, UEA-1 staining of tissue sections corroborated the concept of a reduced number of mTECs in STAT1-deficient thymi when compared with their WT counterparts (Fig. 1A, *center right panel*). To further scrutinize the apparent reduction in mature mTECs, we determined the number of AIRE$^+$ cells in the areas of the thymus characterized by high expression levels of epithelial cell adhesion molecule (EpCAM), a cell-surface marker upregulated during mTEC maturation (28). Thymi from STAT1-deficient mice exhibited clearly reduced numbers of AIRE$^+$ cells compared with those from WT mice (Fig. 1A, *right panel*, quantitated in Fig. 1D). In addition to UEA-1^{hi}, mature mTECs are also characterized by high expression levels of CD80 and MHC class II (MHC II). Stromal cells derived from the thymi of WT and STAT1$^{-/-}$ mice were purified and stained for the indicated markers (Fig. 1E). As anticipated, we noted significantly reduced numbers of UEA-1^{hi}MHC II^{hi} cells as well as AIRE$^+$EPCAM$^+$ cells (Fig. 1E, *left and center panels*; quantitated in Fig. 1F) and CD80$^+$MHC II^{hi} cells (not shown) in STAT1-deficient animals. However, when gated specifically on UEA-1^{hi} cells, no difference in CD80$^+$MHC II^{hi} cells was seen between WT and STAT1$^{-/-}$ mice (Fig. 1E, right). Similar alterations were seen in the mTEC populations of IFNAR1$^{-/-}$ mice, but not IFNGR$^{-/-}$ animals (data not shown). In summary, these findings illustrate that STAT1 or IFNAR1 deficiency diminishes the number of mature AIRE-expressing mTECs and suggest a novel function for type I IFNs in thymic development.

mTECs are recognized for the promiscuous, AIRE-dependent expression of tissue-restricted self-Ag–encoding genes. Because the thymi of STAT1- or IFNAR1-deficient mice contain fewer AIRE-expressing cells, we evaluated the relative levels of two mTEC specific self-Ags, in which expression of one depends on AIRE (Insulin 2), but the other is AIRE independent (C-reactive protein) (1). Analysis of mRNAs from WT or STAT1$^{-/-}$ thymic stromal cells uncovered decreased transcripts for both INS and CRP in STAT1-deficient stromal cells (Fig. 2A). Importantly, we also observed concomitantly reduced AIRE mRNA levels in STAT1$^{-/-}$ epithelial cells, confirming our previous flow cytometric and histological studies (Fig. 2A). These data support the concept that diminished mTEC numbers rather than a reduction of cellular AIRE expression are responsible for the attenuated self-Ag expression in the absence of STAT1. Together, these findings

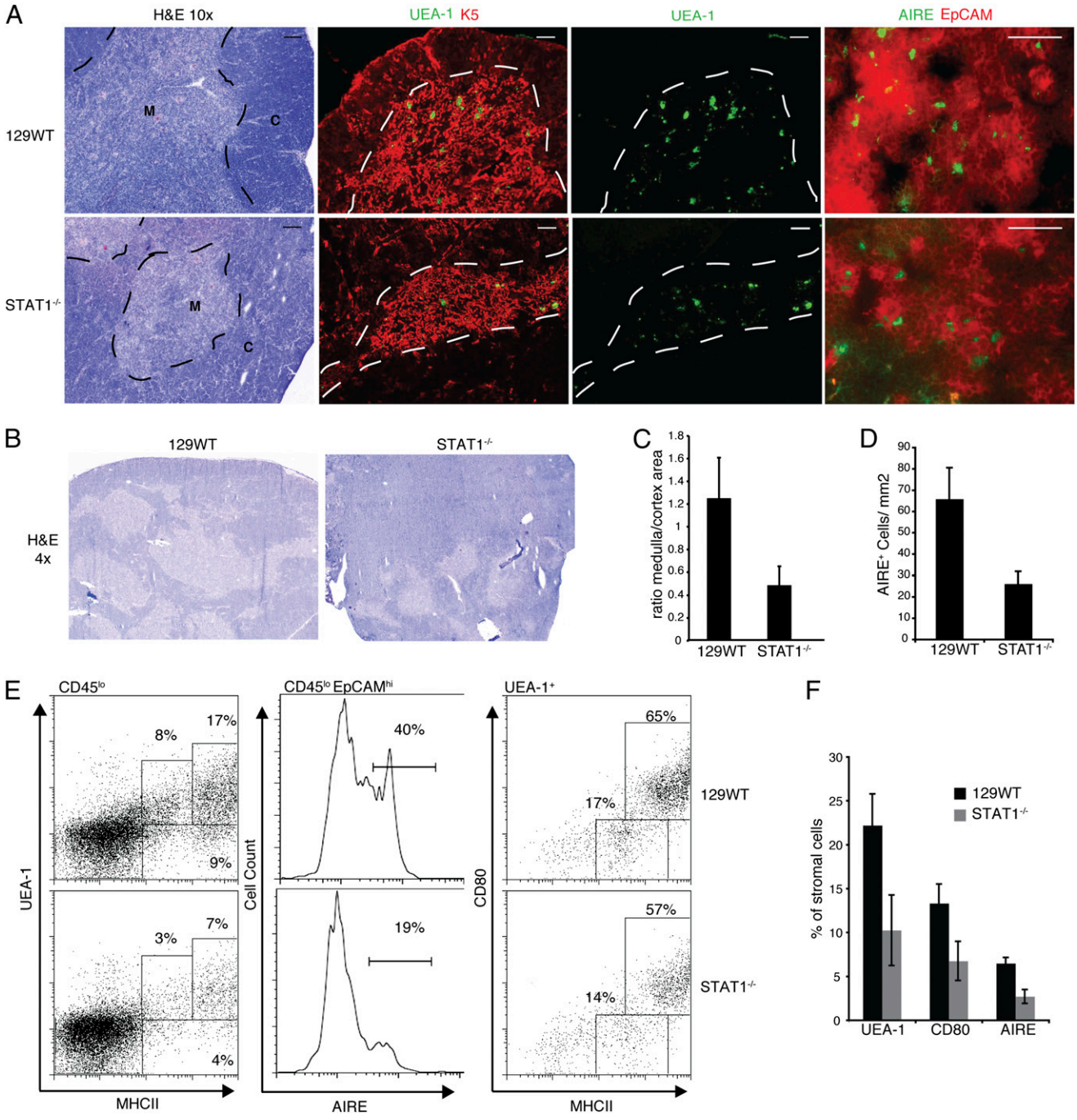

FIGURE 1. Impaired medullary thymic architecture in IFNAR$^{-/-}$ and STAT1$^{-/-}$ mice. (**A**) Thymic architecture in WT129 and STAT1$^{-/-}$ mice as revealed by H&E staining of thymic sections (*left panel*). K5 (red) and UEA-1 (green) staining (*middle panels*). Scale bars, 100 μm. EpCAM (red) and AIRE (green) staining (*right panel*). Scale bars, 50 μm. (**B**) Low original magnification (×4) of H&E stains. (**C**) Ratio of medullary to cortical cellularity in thymic sections from WT and STAT1$^{-/-}$ mice (data collected using ImageJ [National Institutes of Health] and represent average ± SD of three sections each from three mice) ($p < 0.05$). (**D**) AIRE^{+} cells per unit area [quantified from thymus sections shown in (A), *bottom panel*]. (**E**) mTEC populations in WT and STAT1$^{-/-}$ thymi as determined by flow cytometric expression analysis of MHC II and UEA-1 (*left panel*), as well as AIRE and EpCAM (*middle panel*) on CD45^{lo} stromal cells, and MHC II and CD80 expression on UEA-1^{hi} gated stromal cells (*right panel*). (**F**) mTEC populations in WT and STAT1$^{-/-}$ thymi ($n = 4$) using the indicated markers. C, Cortex; M, medulla.

demonstrate a vital contribution of the IFN-α/β–STAT1 axis in the functional development of self-Ag–expressing mTECs.

IFN-β control over RANK signaling is required to maintain AIRE levels in thymic stromal cells

The TNF family members LTβ, CD40, and RANK all contribute the development of mTECs, and deletion of any of the genes encoding these cell-surface molecules or their downstream effectors results in defects of medullary development. As a cross talk between the RANK ligand (RANKL) and IFN signaling pathways had been demonstrated previously in the maturation process of osteoclasts (29), we elected to investigate RANK signaling in thymic stromal cells. Similar to osteoclasts, treatment of freshly isolated thymic stromal cells or the mTEC cell line TE-71 with RANKL resulted in the induction of IFN-β mRNA expression (Fig. 2B). In accordance with previous reports, mTECs rapidly

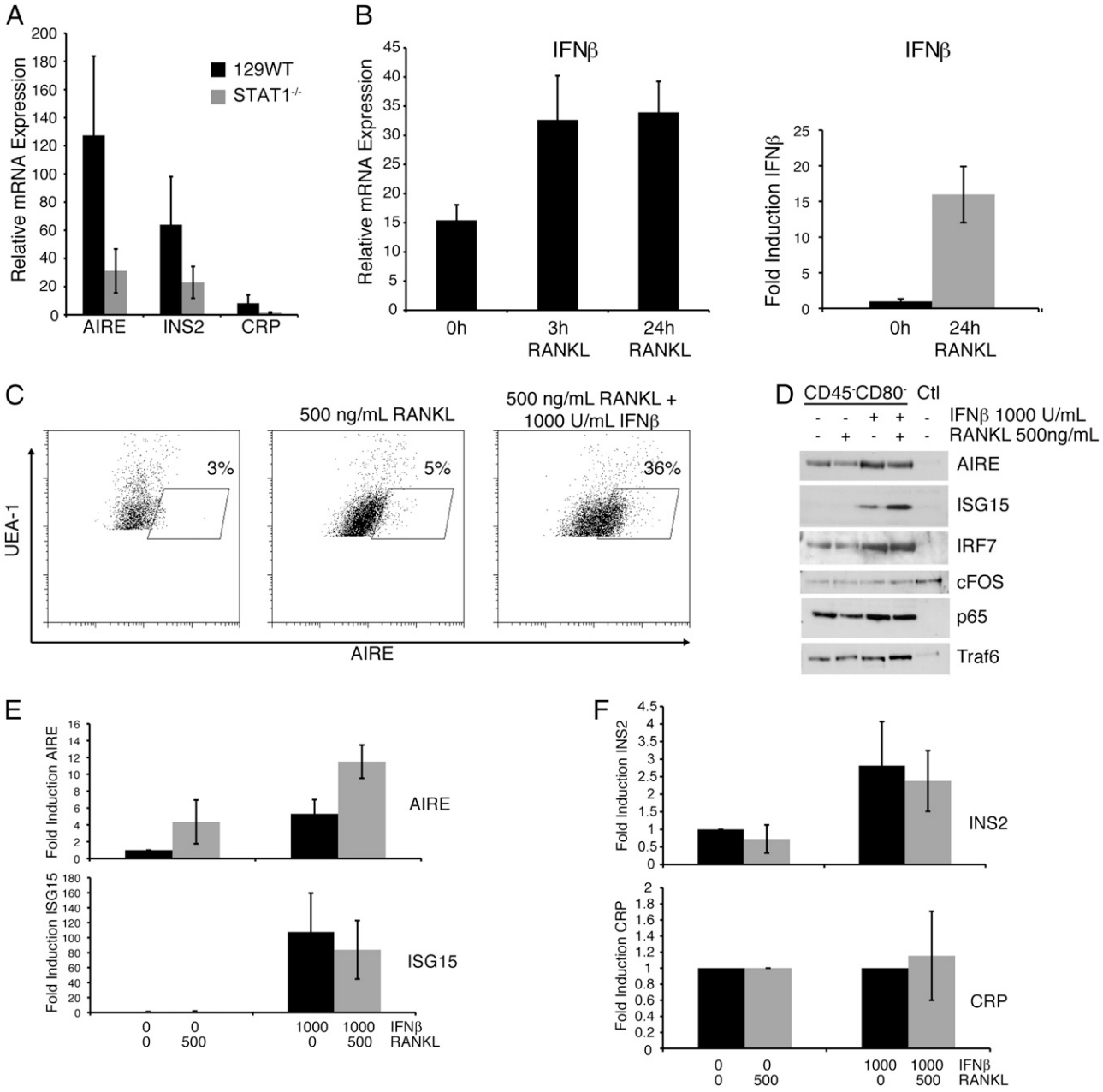

FIGURE 2. IFN-β promotes AIRE expression following RANKL stimulation. (**A**) AIRE, INS2, and CRP mRNA levels in thymic stromal cells from WT and STAT1$^{-/-}$ mice (average ± SD; $n = 4$). (**B**) Thymic epithelial cells from WT mice (*left panel*) or TE-71 cells (*right panel*) were stimulated with 500 ng/ml RANKL for the indicated times and IFN-β mRNA levels were determined by quantitative PCR (qPCR) ($n = 4$). (**C**) Thymic epithelial cells were left untreated or pretreated with 1000 U/ml IFN-β prior to stimulation with 500 ng/ml RANKL for 24 h. UEA-1^{+} cells were analyzed for intracellular AIRE expression by flow cytometry. (**D**) Thymic epithelial cells were depleted of CD80^{+} cells and then stimulated with 500 ng/ml RANKL, 1000 U/ml IFN-β, or both for 24 h. Lysates were probed for AIRE, ISG15, IRF7, cFOS, p65, and Traf6 by Western blotting (representative of three experiments). (**E**) TE-71 cells were treated as indicated, and mRNA levels for AIRE and ISG15 were determined by qPCR (average ± SD; $n = 3$). (**F**) Thymic epithelial cells were treated as indicated and mRNA levels for CRP and INS2 were determined by qPCR (average ± SD; $n = 4$).

lose AIRE expression in culture (Fig. 2C, *left panel*) as determined by intracellular staining for AIRE and flow cytometric analysis. Although RANKL treatment alone of thymic stromal cells slightly increased the number of UEA-1^{hi} cells (Fig. 2C, *middle panel*), costimulation with both IFN-β and RANKL resulted in a pronounced increase in AIRE^{+} cells (Fig. 2C, *right panel*). IFN-β by itself was capable of inducing AIRE expression in both thymic stromal cells (Fig. 2D) as well as in the TE-71 cells (Fig. 2E). In addition, costimulation with IFN-β and RANKL did not result in a reduction of c-fos, p65, or Traf6 (Fig. 2D), indicating that IFN is not causing the degradation of components of the RANK signal transduction pathway in mTECs. This presents a contrast to the mechanism of RANKL and IFN-β opposition during osteoclast differentiation, in which IFN-β treatment causes the loss of c-fos induction by RANKL (29). Finally, analysis of self-Ag expression following stromal cell stimulation indicates that IFN alone can induce expression of the AIRE-dependent self-Ag INS2 (Fig. 2F, *top panel*), but had little effect on the expression of the AIRE-independent self-Ag CRP (Fig. 2F, *bottom panel*). These findings not only demonstrate that IFN-β is induced by RANK signaling on thymic stromal cells, but also that a cross talk exists between the RANK- and

IFNAR-initiated signaling pathways that governs AIRE expression in the thymus.

Previously selected CD4$^+$ T cells are required to promote mTEC development through RANKL expression (6). As STAT1$^{-/-}$ T cells were unable to restore impaired mTEC development in RAG$^{-/-}$ mice in complementation chimera assays (data not shown), we reasoned that RANKL expression on activated thymocytes might be influenced by STAT1 and that consequently a T cell–intrinsic defect might contribute to the impaired development of the medullary compartment in the thymi of IFNAR1$^{-/-}$ and STAT1$^{-/-}$ mice. Using OTII-transgenic mice with Ag specificity toward OVA-derived peptides, we exposed WT thymic stromal cells to OVA peptide and cocultured them with either WT or STAT1$^{-/-}$ OTII$^+$ thymocytes. Twenty-four hours following culture initiation, RANKL expression on thymocytes was analyzed by flow cytometry. As illustrated in Supplemental Fig. 1, activation of both WT and STAT1-deficient thymocytes resulted in increased RANKL expression on their cell surface; however, high levels of RANKL were only ob-

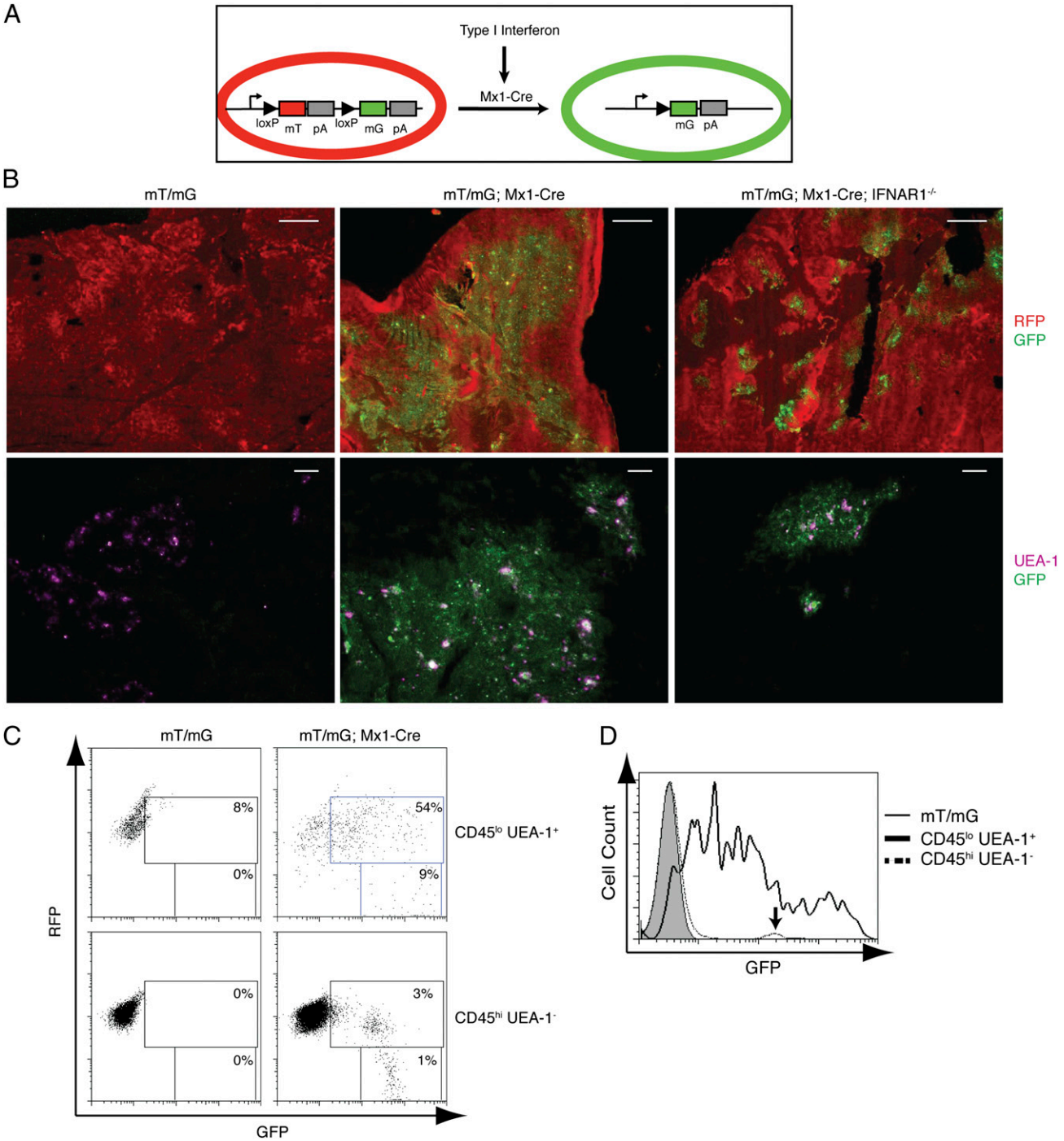

FIGURE 3. Constitutive IFN signaling in the thymus is restricted to the medullary region. (**A**) Schematic diagram of the IFN response reporter mice. IFN-dependent Cre expression results in the excision of the mT sequence coding RFP and expression of mG encoding GFP [Muzumdar et al. (30)]. (**B**) RFP and GFP expression in sections of thymi from WT and IFNAR1$^{-/-}$ mice carrying mT/mG and Mx1-Cre transgenes (*top panel*; scale bars, 500 μm). Sections were also stained for UEA-1 (*bottom panel*, pseudocolored purple; scale bars, 100 μm). (**C**) Flow cytometric analysis of CD45^{lo}UEA-1$^+$ mTEC cells (*top panel*) and CD45^{hi}UEA-1$^-$ hematopoietic cells (*bottom panel*) from thymi of either Mx1-Cre$^-$ or Mx1-Cre$^+$ mT/mG mice. (**D**) Histogram comparing GFP expression levels in CD45^{lo}UEA-1$^+$ mTECs of Mx1-Cre$^-$ or Mx1-Cre$^+$ mT/mG mice. Arrow indicates GFP levels in CD45^{hi} hematopoietic cells.

served in WT thymocytes (Supplemental Fig. 1, *bottom right panel*). Consequently, the failure of mature STAT1$^{-/-}$ T cells to support the development of mTECs in RAG$^{-/-}$ chimeras is likely due to their inability to express sufficient levels of RANKL upon activation. In summary, these observations imply both a T cell–intrinsic and –extrinsic role for STAT1 in mTEC development and function.

Constitutive IFN signaling in the thymic medulla

The phenotype observed in STAT1$^{-/-}$ and IFNAR$^{-/-}$ animals is highly indicative of tonic IFN-α/β signaling in the thymus even in the absence of infectious events. Indeed, IFN-β expression in the thymus had been reported and suggested that type I IFN signaling might be taking place in the thymus. To determine the exact compartment in which IFN signaling occurs in the thymi of uninfected, nonimmunized animals, we devised a transgenic reporter mouse strain. There, a tandem red fluorescent protein (RFP) called tdTomato is followed by a stop codon and a subsequent EGFP-coding region (30). LoxP sites flank the tdTomato gene including the stop codon such that expression of Cre recombinase results in the excision of the tdTomato-coding sequence and the stop codon, releasing expression of the downstream GFP. We crossed these animals to mice harboring the *Cre* transgene under the control of the type I IFN-inducible Mx-1 promoter, which has been widely used to inducibly delete LoxP-flanked alleles by treating mice with either IFN-β or the IFN-inducing TLR3 ligand polyinosinic-polycytidylic acid (31). Conceptually, all cells in these animals display red fluorescence until exposure to type I IFN leads to their transition into green fluorescence (Fig. 3A). Analysis of these double-transgenic mice (mT/mG; Mx1-Cre) revealed the abundant, Mx1-Cre transgene-dependent emergence of GFP-positive cells in the thymic medulla, but not in the cortical region (Fig. 3B, *top middle panel*), indicating that constitutive IFN signaling in the thymus is highly restricted to the thymic medulla. As anticipated, further immunohistochemical analysis detected UEA-1–positive mTECs only among the GFP-positive cell population (Fig. 3B, *bottom panel*, and Fig. 3C). Fig. 3C illustrates that CD45^{lo}UEA-1^{hi} cells express a wider range of GFP as compared with CD45^{hi} cells that display one uniform peak (indicated by arrow) on histograms for GFP expression (Fig. 3D). Unexpectedly, only a very small fraction of thymic T cells expressed GFP in double-transgenic mice (Supplemental Fig. 2, *middle panel*), prompting us to analyze the expression levels of the IFN receptor during thymocyte development. Intriguingly, we observed that both double- and single-positive thymocytes expressed reduced levels of IFNAR1 on their surface (Supplemental Fig. 3A) as compared with CD4 or CD8 single-positive splenocytes. This finding offers an explanation for the previously reported reduced ability of thymocytes to respond to type I IFNs (32). Accordingly, thymocytes do not exhibit the same responsiveness to IFN-β stimulation as splenic T cells, as revealed by reduced phosphorylation of STAT1 (Supplemental Fig. 3B). Thus, although apparently significant amounts of IFN are being produced in the thymic medulla, only the thymic stromal cells, but not thymocytes, are capable of responding to it. mTECs exhibit promiscuous gene expression through AIRE, which could be an alternative explanation to IFN signaling for the expression of the Mx1-Cre transgene in the medulla. Indeed, Mx-1 Cre was suggested to exhibit "leaky" expression (31, 33). To verify that tdTomato excision and subsequent GFP expression in double-transgenic mice was dependent on IFN signaling rather than promiscuous, AIRE-mediated Mx1-Cre expression, we bred the double-transgenic mice onto an IFNAR1$^{-/-}$ background. Elimination of IFNAR1 in mT/mG; Mx1-Cre mice resulted in a dramatic reduction in the number of GFP-positive mTECs (Fig. 3B, *right panels*). In accordance, fewer UEA-1–positive cells were detected in the absence of IFNAR1 (compare Fig. 3B, *bottom middle* and *bottom right panels*). The fact that a few residual GFP-expressing cells can be identified in IFNAR1$^{-/-}$ thymi could possibly be attributed to signaling via the IFN-λ receptor, which is expressed in cells of the epithelial lineage and shares signaling mediators such as STAT1 and -2 with IFNAR1. Thus, even though type I IFNs are predominantly responsible for thymic Mx1-Cre expression, the possibility remains that mTEC-specific Mx1-Cre expression might also occur as a consequence of minute IFN-λ– or AIRE-initiated events, albeit in a significantly less competent manner. Importantly, no GFP^{+} cells were detected among the thymocyte population or in the periphery of mT/mG; Mx1-Cre; IFNAR1$^{-/-}$ mice (Supplemental Fig. 2, *bottom panel*, and data not shown), demonstrating that Mx1-Cre expression in lymphocytes was dependent on type I IFN signaling.

RANKL induces IFN-β expression in UEA-1^{+} mTECs

To identify the cellular sources of IFN-β, the type I IFN commonly produced first, we used knockin mice that express yellow fluorescent protein (YFP) from a bicistronic IFN-β:YFP mRNA (34). Flow cytometric analysis of YFP expression in total cells from thymus of naive IFN-β$^{MOB/MOB}$ mice revealed that ~6% of thymocytes constitutively express IFN-β (Fig. 4, *top panel*). The vast majority of the YFP^{+} cells were characterized as UEA-1^{+} and

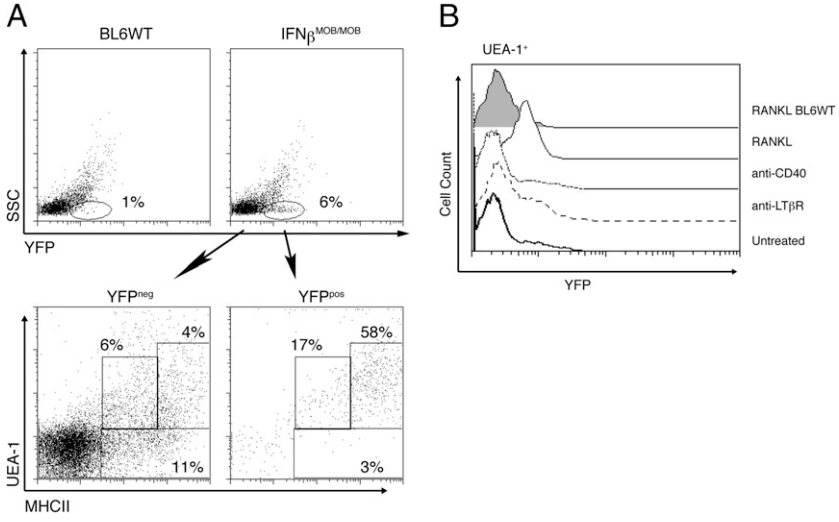

FIGURE 4. IFN-β production by UEA-1^{hi} mTECs. (**A**) Flow cytometric analysis of YFP expression in total cells from thymus of WT (*top left panel*) or IFN-β$^{MOB/MOB}$ mice (*top right panel*). *Bottom panel* shows UEA-1 and MHC II expression in YFP^{-} (*left panel*) and YFP^{+} (*right panel*) cells in thymi of IFN-β$^{MOB/MOB}$ mice. (**B**) Stromal cells were purified from thymi of IFN-β$^{MOB/MOB}$ mice and treated with anti-CD40 (1:100 dilution of supernatant), anti-LTβ receptor (500 ng/ml), or RANKL (500 ng/ml) for 24 h. Histogram illustrates IFN-β:YFP expression in UEA-1^{+} cells following the indicated treatments. Data are representative of three separate experiments.

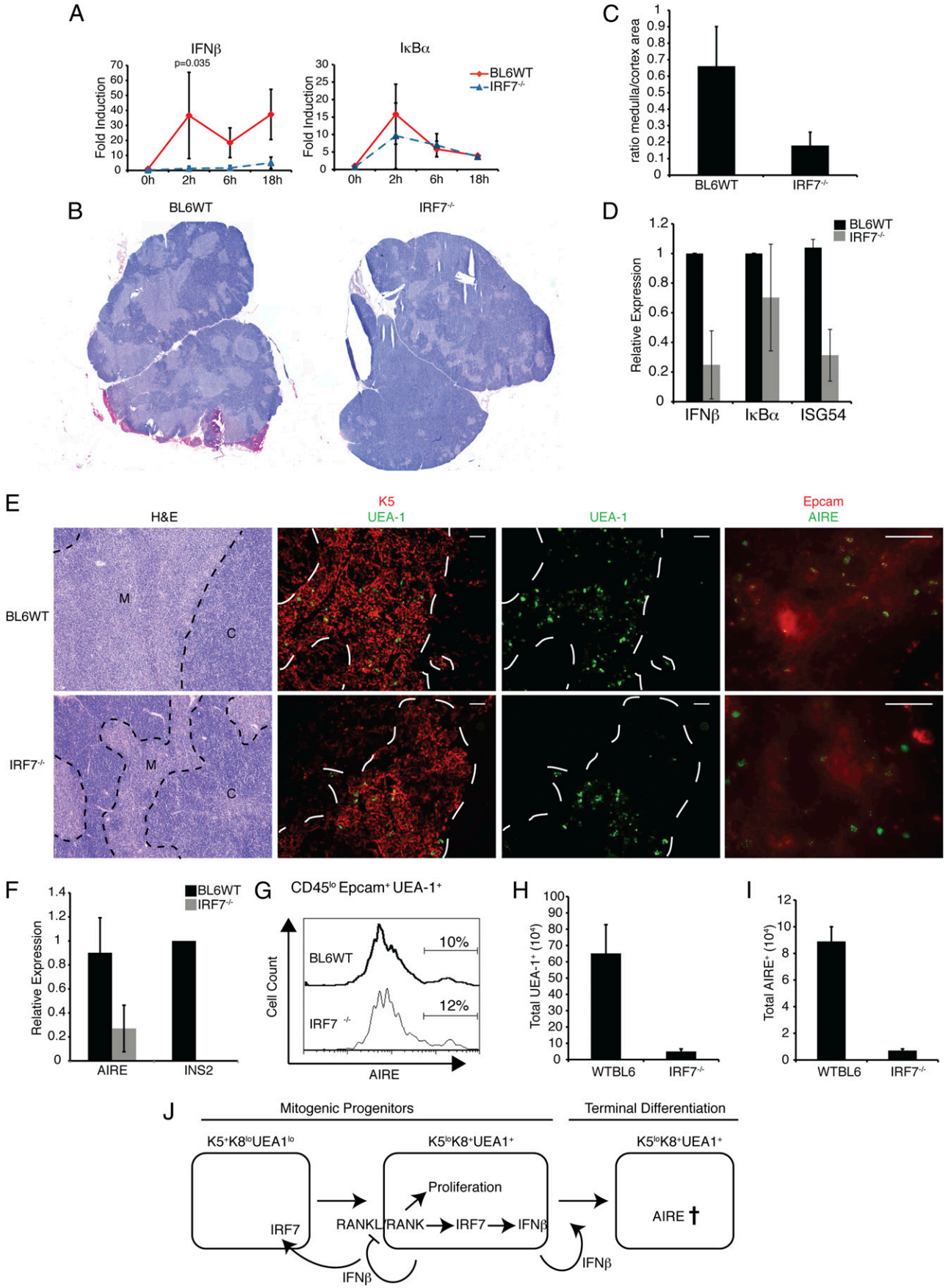

FIGURE 5. IRF7 is necessary for thymic IFN-β expression and mTEC development. (**A**) Thymic stromal cells from WT or IRF7$^{-/-}$ mice were purified and stimulated with 500 ng/ml RANKL for the indicated time points. Expression of IFN-β and IκBα mRNAs was determined by quantitative PCR (qPCR). (**B**) Thymic architecture in WT and IRF7$^{-/-}$ mice revealed by H&E staining of thymic sections (scale bar, 500 μm). (**C**) Ratio of medullary to cortical cellularity in thymic sections from WT and IRF7$^{-/-}$ mice (data collected using ImageJ [National Institutes of Health] and (*Figure legend continues*)

MHC II^{high} cells (Fig. 4A, *bottom panel*), consistent with our hypothesis that AIRE$^-$ immature mTECs are the major source of type I IFN in the thymus. As previously indicated, IFN-β is typically produced by plasmacytoid dendritic cells and other cell types after recognition of pathogen-associated molecular patterns via pattern recognition receptors. However, IFN-β production by UEA-1$^+$ mTECs occurs independent of such stimulation, thus raising the question as to the identity of the factor(s) that control type I IFN release in the thymus. To this end, thymic stromal cells were purified from thymus of IFN-β$^{MOB/MOB}$ mice and treated with RANKL for 24 h. As shown in Fig. 4B, a clear upregulation of YFP expression in response to RANKL could be observed in UEA-1$^+$ mTECs, consistent with our earlier findings illustrated in Fig. 2B. In contrast, no induction of YFP:IFN-β was noticeable when the cells were stimulated through CD40 or the LTβ receptor (Fig. 4B), indicating that RANKL is indeed responsible for the presence of IFN-β in the thymic medulla.

IRF7-deficient mice display defects in mTEC development and IFN-β expression after RANK stimulation

Our results demonstrated a need for tonic IFN-α/β signaling in promoting the development and maturation of AIRE$^+$ mTECs, and revealed that UEA-1$^+$AIRE$^-$ immature mTECs are the primary source of IFN-β in the thymus. Previous work with osteoclasts demonstrated that IFN-β production following RANK signaling was dependent on c-Fos and independent of the expression of IRFs (29). However, no IRF7$^{-/-}$ cells were employed in that study, and in light of the fact that IRF3 and -7 are required for induction of IFN-β in response to pathogens, we decided to investigate IFN production following RANKL stimulation in mTECs derived from IRF3- and IRF7-deficient mice. As shown in Fig. 5A, IRF7-deficient thymic stromal cells were incapable of inducing IFN-β messages following RANKL stimulation, whereas significant IFN-β messages could be induced in WT cells (Fig. 5A, *left panel*; $p < 0.05$) or IRF3-deficient stroma (not shown). Furthermore, no difference in the RANK signaling pathway leading up to induction of IκBα was observed (Fig. 5A, *right panel*; $p > 0.05$). Thus, IRF7 appears necessary for IFN production in response to RANKL stimulation in the thymus.

Based on the above findings, it seemed reasonable to expect that the loss of IRF7 would have a detrimental impact on the mTEC population. Indeed, H&E staining revealed a clear reduction in the thymic medullary region in IRF7-deficient mice as compared with WT animals (Fig. 5B), which is highlighted by a significant alteration of the mTEC/cortical TEC (cTEC) ratio (Fig. 5C). Accordingly, we noted a reduction in the IFN signature in freshly isolated thymic stroma (Fig. 5D). Immunostaining for K5 indicated the presence of immature mTECs in the IRF7-deficient thymus; however, there was a drastic reduction in the number of UEA-1$^+$ cells (Fig. 5E, *middle panels*), with a concomitant diminution of mature AIRE$^+$ cells (Fig. 5E, *right panel*). Accordingly, total stromal cells isolated from IRF7$^{-/-}$ thymi contained lower levels of AIRE mRNA, accompanied by a severe reduction in the expression of the AIRE-dependent self-Ag INS2 (Fig. 5F). Flow cytometric analysis of the few remaining mature mTECs revealed that the amount of AIRE protein in the IRF7$^{-/-}$ cells is identical to that found in their WT counterparts (Fig. 5G). However, the total numbers of UEA-1$^+$ and AIRE$^+$ cells were dramatically reduced in the thymi of IRF7$^{-/-}$ mice compared with those of WT animals (Fig. 5H, 5I). Thus, we conclude that the lack of IFN-β production by IRF7$^{-/-}$ stromal cells illustrated in Fig. 5A is the result of severely diminished numbers of the IFN-β–producing cells.

In summary, our findings indicate that mTECs experience a hindrance in the progression from the immature K14$^+$K5^{hi}UEA-1$^-$ population to mature UEA-1$^+$ and subsequently AIRE expressing cells in the absence of IRF7. We find that the presence of IRF7 is required in order for RANKL to facilitate the production of IFN-β, which in turn is crucial for the differentiation of immature mTECs into mature AIRE$^+$ cells capable of promiscuous self-Ag expression.

Discussion

Our previous work demonstrated that STAT1 deficiency dramatically increases the incidence of autoimmune disease (18). In addition to decreased CD4$^+$CD25$^+$ T$_{reg}$ function, it seemed conceivable that the absence of STAT1 also leads to impaired deletion of autoreactive T cells in the thymus. Indeed, we found that both STAT1 and the type I IFN receptor chain IFNAR, but not the IFNGR, are crucial for the processes governing the deletion of autoreactive CD8$^+$ cells in the TCR^{HY} model system (22). Importantly, we discovered that the coexistence of WT thymocytes restored the impaired elimination of TCR^{HY}STAT1$^{-/-}$ thymocytes in male bone marrow chimeric mice, whereas bone marrow of TCR$^{-/-}$ mice that lack mature T cells failed to support the purging of the autoreactive TCR^{HY}STAT1$^{-/-}$ T cells, thus strongly supporting the notion that mature T cells contribute to the efficiency of the selection process in a STAT1-dependent manner. It is of interest to note that a similar effect was described in mice lacking CD40 (35). Specifically, it was shown that CD40L plays a non–cell-intrinsic role in deletion of self-reactive thymocytes. Although the molecular mechanism behind this effect was not known at the time, we now know that CD40 plays a role in mTEC development (26). As development of mTECs, which exhibit a short $t_{1/2}$ (36) and are indispensible for negative selection of self-reactive T cells, is dependent on their T cell interactions, we decided to analyze the architecture of STAT1$^{-/-}$ thymi. Indeed, STAT1$^{-/-}$ mice display a reduced medullary compartment as well as a reduction in the number of mature mTECs expressing CD80, UEA-1, and AIRE (Fig. 1). The defects in mTEC development in STAT1$^{-/-}$ mice were strikingly similar to defects found in the absence of the TNF family members RANK, CD40, and LTβ (7, 8, 26). The importance of cross-talk between the RANK and IFN signaling cascades had previously been described in osteoclast differentiation and maturation (29). There, RANKL presented by mature T cells stimulates RANK on osteoclast precursors, resulting in their proliferation and simultaneous production of IFN-β. Autocrine stimulation via IFNAR subsequently leads to the

represent average ± SD of three sections each from three mice) ($p < 0.05$). (**D**) mRNA levels of IFN-β, IκBα, and ISG54 in thymic stromal cells from WT or IRF7$^{-/-}$ mice as determined by qPCR. (**E**) Thymic architecture in WT and IRF7$^{-/-}$ mice as revealed by H&E staining of thymic sections (*left panel*), K5 and UEA-1 expression (*second panel from left*; scale bars, 100 μm), UEA-1 only (*second panel from right*), as well as EpCAM and AIRE expression (*right panel*; scale bars, 50 μm). (**F**) Relative mRNA levels of AIRE and INS2 in purified stromal cells from WT and IRF7$^{-/-}$ thymi measured by qPCR ($n = 3$). (**G**) Histogram shows percentage of AIRE$^+$ cells in the CD45^{lo}EpCAM$^+$UEA-1^{hi} gate of thymic stromal cells from WT and IRF7$^{-/-}$ mice. (**H**) Total number of UEA-1^{hi} cells as determined by flow cytometric analysis of CD45^{lo}EpCAM$^+$UEA-1^{hi} mTEC populations from WT and IRF7$^{-/-}$ thymi. (**I**) Total number of AIRE$^+$ cells based on flow cytometric analysis of CD45^{lo}EpCAM$^+$UEA-1^{hi}AIRE$^+$ mTEC populations in WT and IRF7$^{-/-}$ thymi ($n = 4$). (**J**) Hypothetical model of IFN-β production and function in the thymus.

termination of RANK signaling, causing the terminal differentiation of the precursors into mature, nonproliferating osteoclasts. We reasoned that a similar interplay might govern the development of thymic epithelial cells. Indeed, we noted that IFN-β is induced by treatment of thymic stromal cells with soluble RANKL. However, addition of exogenous IFN-β was able to promote the maintenance of AIRE expression during RANKL stimulation, consistent with the notion that RANKL promotes expansion of the mTEC population, whereas IFN-β mediates their differentiation and/or survival. In accordance with this concept, we noticed elevated K5 expression (characteristic of UEA-1–negative, immature mTECs) in STAT1-deficient thymi with a parallel reduction in the expression of cell-surface markers associated with mature mTECs (Fig. 1E). We therefore conclude that IFN production following RANK signaling provides a feedback loop that facilitates the terminal differentiation of mTECs, which is impaired in the absence of IFNAR or STAT1. These striking observations offer a new model for the development of medullary thymic epithelia that involves cross talk between the RANK and type I IFN signaling pathways.

Under the above-outlined hypothesis, one has to assume the continuous production of type I IFNs in the thymic medulla independent of infectious processes or other immune-response provoking events. In contrast to IFN-γ, of which the role in T cell development has been studied extensively, comparatively little is known about the contributions of IFN-α/β to this process. We therefore designed an animal model that allows for the identification of cells that have been exposed to type I IFN. By means of this mT/mG; Mx1-Cre system, we observe spatially tightly restricted IFN responses in the thymus that are almost exclusively limited to the medulla (Fig. 3). Our studies using mT/mG; Mx1-Cre mice lacking either IFNAR or STAT1 revealed a dramatic decline of GFP-positive mTECs compared with thymi from mice with an intact IFN-α/β signaling cascade, corroborating the vital contributions of this cytokine to the development of the thymic medullary compartment. Intriguingly, IFNAR$^{-/-}$ reporter mice still exhibited some GFP expression in the remaining UEA-1^{+} cells. One possible explanation might be redundancy to type I IFN signaling in mTECs, as epithelial cells in general are responsive to IL-29 (IFN-λ). Although IFN-λ signals through a receptor distinct from IFNAR1/2, it also employs STAT1/2 heterodimers and stimulates an overlapping gene profile (37). Nevertheless, such IFN-λ expression in the thymus is apparently insufficient to promote mTEC maturation in IFNAR$^{-/-}$ mice (Figs. 1, 3). Alternatively, an IRF family member could be mediating residual expression of Mx1-Cre in IFNAR$^{-/-}$ mice. In support of our model, a search of the public Gene Expression Omnibus profiles database indicates a strong IFN signature in mTECs as compared with cTECs. In fact, many of the markers used to identify mature mTEC such as CD80, CD86, and MHC II are IFN-stimulated genes. Interestingly, microarray profiles of purified mTECs revealed that CD80^{hi} mTEC exhibit a reduction in both components of IFN signaling as well as a reduction in IFN-stimulated genes as compared with CD80^{lo} mTECs, which may be an indication of chronic IFN exposure of mature differentiated CD80^{hi} mTECs.

Consistent with our findings, the production of IFN in the thymus has recently also been described through the use of a luciferase transgene inserted into the IFN-β gene locus (38). In these animals, luciferase activity was linked to AIRE expression (38). Although it was possible that IFN-β is a direct target of AIRE-controlled transcription, the absence of AIRE results in a misdirection of mTEC development as noted in AIRE-deficient animals (27). Our studies indicate that the main IFN-β–producing cells in the thymus are UEA-1^{+} cells, regardless of AIRE expression (Fig. 4A).

In an effort to identify the factors controlling IFN-β production in the thymus, we discovered that IRF7 is not only eliciting IFN expression downstream of RANK, but also that IRF7-deficient mice harbor severe defects in mTEC development (Fig. 5). As IRF3$^{-/-}$ mice were found to have normal thymic compartments and IFN-β production, this represents only the second instance of an IRF7/IRF3-independent induction of IFN-β, the other involving pathogen-associated molecular pattern–stimulated plasmacytoid dendritic cells (25). Further studies will be aimed to elucidate the pathways involved in IRF7 activation downstream of RANK as well as the consequences of the loss of IRF7 in terms of T cell tolerance and autoimmunity.

Taken together, the data presented in this study illustrate a complex interplay between mature and developing T lymphocytes and mTECs that involves RANK and type I IFN signaling. There are persistent controversies on the exact stages mTECs progress through during their development and maturation. A common model holds that K5^{+}keratin 8 (K8)$^{+}$UEA-1^{-} common precursors develop into K5^{-}K8^{+}UEA-1^{-} cTECs and the major mTEC population characterized as K5^{+}K8^{-}UEA-1^{-}. A small population progresses into medullary K5^{-}K8^{+} cells that start to express UEA-1 and eventually AIRE (39). Our data are consistent with the notion that IFN-β produced by UAE-1^{+} cells acts on K5^{+}K8^{+} UEA-1^{-} precursors to promote their upregulation of IRF7 and progression into UAE-1^{+} cells, thus explaining the diminution of UAE-1^{+} cells in mice lacking IRF7, IFNAR, or STAT1. In addition, IFN-β likely also functions in an autocrine feedback loop, terminating the RANK signaling and facilitating the upregulation of AIRE in terminally differentiated UAE-1^{+} cells (Fig. 5J).

As IFNAR-, STAT1-, and IRF7-deficient mice have been frequently used to assess the role of the type I IFN system in antiviral defense, our new findings might also merit a re-evaluation of the conclusions drawn from these studies, as failure to clear distinct infections might be due to altered T cell populations at the onset of the experiment rather than a sole function of IRF7/IFN/STAT1 in the innate immune response. Lastly, our findings might have additional implications due to the fact that many viruses are capable of inhibiting IFN signaling and thus evading the immune response. Therefore, viruses that infect thymic cell populations might evoke immune disorders by repressing IFN signaling in medullary thymic stromal cells, consequently breaking tolerance of self-reactive thymocytes or upsetting T_{reg} development.

Acknowledgments

We thank Drs. A. Farr, A. Goldrath, S. Hedrick, E. Zuniga, and R. Rickert for many helpful discussions and advice.

Disclosures

The authors have no financial conflicts of interest.

References

1. Anderson, M. S., E. S. Venanzi, L. Klein, Z. Chen, S. P. Berzins, S. J. Turley, H. von Boehmer, R. Bronson, A. Dierich, C. Benoist, and D. Mathis. 2002. Projection of an immunological self shadow within the thymus by the aire protein. *Science* 298: 1395v1401.
2. Liston, A., S. Lesage, J. Wilson, L. Peltonen, and C. C. Goodnow. 2003. Aire regulates negative selection of organ-specific T cells. *Nat. Immunol.* 4: 350–354.
3. Finnish-German, A. C.; Finnish-German APECED Consortium. 1997. An autoimmune disease, APECED, caused by mutations in a novel gene featuring two PHD-type zinc-finger domains. *Nat. Genet.* 17: 399–403.
4. Peterson, P., K. Nagamine, H. Scott, M. Heino, J. Kudoh, N. Shimizu, S. E. Antonarakis, and K. J. Krohn. 1998. APECED: a monogenic autoimmune disease providing new clues to self-tolerance. *Immunol. Today* 19: 384–386.
5. Ramsey, C., O. Winqvist, L. Puhakka, M. Halonen, A. Moro, O. Kämpe, P. Eskelin, M. Pelto-Huikko, and L. Peltonen. 2002. Aire deficient mice develop multiple features of APECED phenotype and show altered immune response. *Hum. Mol. Genet.* 11: 397–409.

6. Hikosaka, Y., T. Nitta, I. Ohigashi, K. Yano, N. Ishimaru, Y. Hayashi, M. Matsumoto, K. Matsuo, J. M. Penninger, H. Takayanagi, et al. 2008. The cytokine RANKL produced by positively selected thymocytes fosters medullary thymic epithelial cells that express autoimmune regulator. *Immunity* 29: 438–450.
7. Dunn, R. J., C. J. Luedecker, H. S. Haugen, C. H. Clegg, and A. G. Farr. 1997. Thymic overexpression of CD40 ligand disrupts normal thymic epithelial organization. *J. Histochem. Cytochem.* 45: 129–141.
8. Boehm, T., S. Scheu, K. Pfeffer, and C. C. Bleul. 2003. Thymic medullary epithelial cell differentiation, thymocyte emigration, and the control of autoimmunity require lympho-epithelial cross talk via LTbetaR. *J. Exp. Med.* 198: 757–769.
9. Chin, R. K., J. C. Lo, O. Kim, S. E. Blink, P. A. Christiansen, P. Peterson, Y. Wang, C. Ware, and Y. X. Fu. 2003. Lymphotoxin pathway directs thymic Aire expression. *Nat. Immunol.* 4: 1121–1127.
10. Burkly, L., C. Hession, L. Ogata, C. Reilly, L. A. Marconi, D. Olson, R. Tizard, R. Cate, and D. Lo. 1995. Expression of relB is required for the development of thymic medulla and dendritic cells. *Nature* 373: 531–536.
11. Kajiura, F., S. Sun, T. Nomura, K. Izumi, T. Ueno, Y. Bando, N. Kuroda, H. Han, Y. Li, A. Matsushima, et al. 2004. NF-kappa B-inducing kinase establishes self-tolerance in a thymic stroma-dependent manner. *J. Immunol.* 172: 2067–2075.
12. Akiyama, T., S. Maeda, S. Yamane, K. Ogino, M. Kasai, F. Kajiura, M. Matsumoto, and J. Inoue. 2005. Dependence of self-tolerance on TRAF6-directed development of thymic stroma. *Science* 308: 248–251.
13. David, M. 2002. Signal transduction by type I interferons. *Biotechniques* Suppl: 58–65.
14. Müller, M., C. Laxton, J. Briscoe, C. Schindler, T. Improta, J. E. Darnell, Jr., G. R. Stark, and I. M. Kerr. 1993. Complementation of a mutant cell line: central role of the 91 kDa polypeptide of ISGF3 in the interferon-alpha and -gamma signal transduction pathways. *EMBO J.* 12: 4221–4228.
15. Schindler, C., and J. E. Darnell, Jr. 1995. Transcriptional responses to polypeptide ligands: the JAK-STAT pathway. *Annu. Rev. Biochem.* 64: 621–651.
16. Durbin, J. E., R. Hackenmiller, M. C. Simon, and D. E. Levy. 1996. Targeted disruption of the mouse *Stat1* gene results in compromised innate immunity to viral disease. *Cell* 84: 443–450.
17. Meraz, M. A., J. M. White, K. C. Sheehan, E. A. Bach, S. J. Rodig, A. S. Dighe, D. H. Kaplan, J. K. Riley, A. C. Greenlund, D. Campbell, et al. 1996. Targeted disruption of the Stat1 gene in mice reveals unexpected physiologic specificity in the JAK-STAT signaling pathway. *Cell* 84: 431–442.
18. Nishibori, T., Y. Tanabe, L. Su, and M. David. 2004. Impaired development of CD4+ CD25+ regulatory T cells in the absence of STAT1: increased susceptibility to autoimmune disease. *J. Exp. Med.* 199: 25–34.
19. Karp, C. L., C. A. Biron, and D. N. Irani. 2000. Interferon beta in multiple sclerosis: is IL-12 suppression the key? *Immunol. Today* 21: 24–28.
20. Goverman, J., A. Woods, L. Larson, L. P. Weiner, L. Hood, and D. M. Zaller. 1993. Transgenic mice that express a myelin basic protein-specific T cell receptor develop spontaneous autoimmunity. *Cell* 72: 551–560.
21. Lafaille, J. J., K. Nagashima, M. Katsuki, and S. Tonegawa. 1994. High incidence of spontaneous autoimmune encephalomyelitis in immunodeficient anti-myelin basic protein T cell receptor transgenic mice. *Cell* 78: 399–408.
22. Moro, H., D. C. Otero, Y. Tanabe, and M. David. 2011. T cell-intrinsic and -extrinsic contributions of the IFNAR/STAT1-axis to thymocyte survival. *PLoS ONE* 6: e24972.
23. Müller, U., U. Steinhoff, L. F. L. Reis, S. Hemmi, J. Pavlovic, R. M. Zinkernagel, and M. Aguet. 1994. Functional role of type I and type II interferons in antiviral defense. *Science* 264: 1918–1921.
24. Sakaguchi, S., H. Negishi, M. Asagiri, C. Nakajima, T. Mizutani, A. Takaoka, K. Honda, and T. Taniguchi. 2003. Essential role of IRF-3 in lipopolysaccharide-induced interferon-beta gene expression and endotoxin shock. *Biochem. Biophys. Res. Commun.* 306: 860–866.
25. Honda, K., H. Yanai, H. Negishi, M. Asagiri, M. Sato, T. Mizutani, N. Shimada, Y. Ohba, A. Takaoka, N. Yoshida, and T. Taniguchi. 2005. IRF-7 is the master regulator of type-I interferon-dependent immune responses. *Nature* 434: 772–777.
26. Akiyama, T., Y. Shimo, H. Yanai, J. Qin, D. Ohshima, Y. Maruyama, Y. Asaumi, J. Kitazawa, H. Takayanagi, J. M. Penninger, et al. 2008. The tumor necrosis factor family receptors RANK and CD40 cooperatively establish the thymic medullary microenvironment and self-tolerance. *Immunity* 29: 423–437.
27. Dooley, J., M. Erickson, and A. G. Farr. 2008. Alterations of the medullary epithelial compartment in the Aire-deficient thymus: implications for programs of thymic epithelial differentiation. *J. Immunol.* 181: 5225–5232.
28. Farr, A., A. Nelson, J. Truex, and S. Hosier. 1991. Epithelial heterogeneity in the murine thymus: a cell surface glycoprotein expressed by subcapsular and medullary epithelium. *J. Histochem. Cytochem.* 39: 645–653.
29. Takayanagi, H., S. Kim, K. Matsuo, H. Suzuki, T. Suzuki, K. Sato, T. Yokochi, H. Oda, K. Nakamura, N. Ida, et al. 2002. RANKL maintains bone homeostasis through c-Fos-dependent induction of interferon-beta. *Nature* 416: 744–749.
30. Muzumdar, M. D., B. Tasic, K. Miyamichi, L. Li, and L. Luo. 2007. A global double-fluorescent Cre reporter mouse. *Genesis* 45: 593–605.
31. Kühn, R., F. Schwenk, M. Aguet, and K. Rajewsky. 1995. Inducible gene targeting in mice. *Science* 269: 1427–1429.
32. Marino, J. H., C. J. Van De Wiele, J. M. Everhart, R. Masengale, R. J. Naukam, M. J. Schniederjan, S. Vo, and T. K. Teague. 2006. Attenuation of cytokine responsiveness during T cell development and differentiation. *J. Interferon Cytokine Res.* 26: 748–759.
33. Chan, I. T., J. L. Kutok, I. R. Williams, S. Cohen, L. Kelly, H. Shigematsu, L. Johnson, K. Akashi, D. A. Tuveson, T. Jacks, and D. G. Gilliland. 2004. Conditional expression of oncogenic K-ras from its endogenous promoter induces a myeloproliferative disease. *J. Clin. Invest.* 113: 528–538.
34. Scheu, S., P. Dresing, and R. M. Locksley. 2008. Visualization of IFNbeta production by plasmacytoid versus conventional dendritic cells under specific stimulation conditions in vivo. *Proc. Natl. Acad. Sci. USA* 105: 20416–20421.
35. Williams, J. A., S. O. Sharrow, A. J. Adams, and R. J. Hodes. 2002. CD40 ligand functions non-cell autonomously to promote deletion of self-reactive thymocytes. *J. Immunol.* 168: 2759–2765.
36. Gray, D., J. Abramson, C. Benoist, and D. Mathis. 2007. Proliferative arrest and rapid turnover of thymic epithelial cells expressing Aire. *J. Exp. Med.* 204: 2521–2528.
37. Sommereyns, C., S. Paul, P. Staeheli, and T. Michiels. 2008. IFN-lambda (IFN-lambda) is expressed in a tissue-dependent fashion and primarily acts on epithelial cells in vivo. *PLoS Pathog.* 4: e1000017.
38. Lienenklaus, S., M. Cornitescu, N. Zietara, M. Łyszkiewicz, N. Gekara, J. Jabłónska, F. Edenhofer, K. Rajewsky, D. Bruder, M. Hafner, et al. 2009. Novel reporter mouse reveals constitutive and inflammatory expression of IFN-beta in vivo. *J. Immunol.* 183: 3229–3236.
39. Klug, D. B., C. Carter, E. Crouch, D. Roop, C. J. Conti, and E. R. Richie. 1998. Interdependence of cortical thymic epithelial cell differentiation and T-lineage commitment. *Proc. Natl. Acad. Sci. USA* 95: 11822–11827.

Supplementary Figure Legends

Suppl. Figure 1: Reduced RankL expression on STAT1-/- thymocytes.

Thymocytes from TCR^{OTII} and $TCR^{OTII}STAT1^{-/-}$ mice were exposed to APCs previously loaded with $Ova^{323-339}$ peptide for 24 hrs and analyzed for RANKL expression (Avg+/-SD; n=3).

Suppl. Figure 2: Reduced IFNα/β responses in Thymocytes

tdTomato (RFP) and GFP expression in the CD4/CD8 double-negative (DN), double-positive (DP) as well as single-positive (SP) CD4 and CD8 thymocyte populations derived from WT (middle panel) and $IFNAR^{-/-}$ mice (lower panel) carrying mT/mG +/- Mx1-Cre transgenes as determined by flow cytometry (plots are representative of three mice each).

Suppl. Figure 3: Reduced IFNAR levels and IFNα/β responses in thymocytes.

a) IFNAR1 receptor expression levels in the indicated thymocyte populations (thin line) compared to splenic T cells (bold line) from WT mice as determined by flow cytometry (histograms are representative of three mice). **b)** Dose response of interferon signaling in thymocytes compared to splenic T cells as evidenced by STAT1 phosphorylation blot. Total STAT1 is shown as loading control.

Suppl. Figure 1

Suppl. Figure 2

Suppl. Figure 3